# Indol-1-yl Acetic Acids as Peroxisome Proliferator-Activated Receptor Agonists: Design, Synthesis, Structural Biology, and Molecular Docking Studies

Neeraj Mahindroo,[†] Chiung-Chiu Wang,[†] Chun-Chen Liao,[‡] Chien-Fu Huang,[†] I-Lin Lu,[†,§] Tzu-Wen Lien,[†] Yi-Huei Peng,[†,◇] Wei-Jan Huang,[‡] Ying-Ting Lin,[†] Ming-Chen Hsu,[†] Chia-Hui Lin,[‡] Chia-Hua Tsai,[†] John T.-A. Hsu,[†,#] Xin Chen,[†] Ping-Chiang Lyu,[◇] Yu-Sheng Chao,[†] Su-Ying Wu,*[,†] and Hsing-Pang Hsieh*[,†]

*Division of Biotechnology and Pharmaceutical Research, National Health Research Institutes, 35, Keyan Road, Zhunan Town, Miaoli County 350, Taiwan, Republic of China, Department of Chemistry, Department of Life Sciences, and Department of Chemical Engineering, National Tsing Hua University, Hsinchu 300, Taiwan, Republic of China, and Graduate Institute of Life Sciences, National Defense Medical Center, Taipei 114, Taiwan, Republic of China*

*Received October 16, 2005*

A series of novel indole-based PPAR agonists is described leading to discovery of **10k**, a highly potent PPAR pan-agonist. The structural biology and molecular docking studies revealed that the distances between the acidic group and the linker, when a ligand was complexed with PPAR$\gamma$ protein, were important for the potent activity. The hydrophobic tail part of **10k** makes intensive hydrophobic interaction with the PPAR$\gamma$ protein resulting in potent activity.

## Introduction

The prevalence of type 2 diabetes mellitus, a multifactorial heterogeneous group of disorders resulting from defects in insulin secretion, insulin action, or both, has increased dramatically over the past several decades.[1] The changes in human environment, behavior, and lifestyle have resulted in escalating rates of both diabetes and obesity.[2] The metabolic syndrome, a deadly quartet of insulin resistance, central obesity, dyslipidaemia, and hypertension, is associated with increased risk of cardiovascular diseases.[3]

The peroxisome proliferator-activated receptors (PPARs) are lipid-activated transcription factors exerting several functions in development and metabolism.[4] They are targets of drugs effective in treatment of metabolic disorders. The modulation of PPAR activity might be an effective therapy for metabolic syndrome including obesity. The three PPAR subtypes, PPAR$\gamma$, PPAR$\alpha$, and PPAR$\delta$, have been the focus of extensive research during past decade.[5] The currently marketed PPAR$\gamma$ agonists have only modest net efficacy and have the potential for several undesired side effects.[6] Novel PPAR ligands are now being developed that possess broader efficacies and improved tolerability compared with currently available therapeutic agents[5] (Figure 1). The lipid-lowering and cardioprotective effect of PPAR$\alpha$ agonists, insulin-sensitizing effect of PPAR$\gamma$ agonists, and fatty acid catabolism by PPAR$\delta$ agonists are well documented.[5−8] The PPAR pan-agonist could represent a significant novel potential drug for the clinical treatment of metabolic disorders.

We have recently reported a series of indole-based PPAR pan-agonists with the lead compound **5** displaying a potent glucose lowering efficacy and an excellent pharmacokinetic profile.[9] In continuation of this work we further explored new

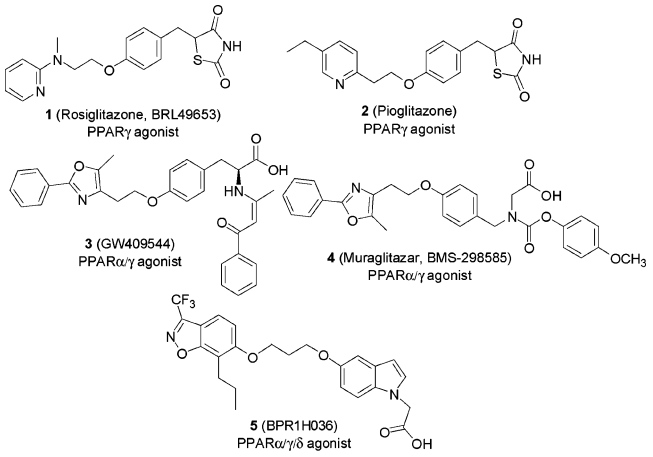


**Figure 1.** PPAR agonists.

hydrophobic building blocks as the tail part of the indole-based PPAR agonists. This article describes the design, synthesis, and structure−activity relationships (SARs) of novel highly potent PPAR$\alpha/\gamma/\delta$ pan-agonists with hydrophobic tails selected from 20 commercially available building blocks, which were further modified to improve the activity. The structural biology and molecular docking studies were carried out to reveal the reasons for variation in potency in 4-, 5-, and 6-substiuted indol-1-yl acetic acids and to predict the structural requirements for the acidic head of PPAR$\gamma$ agonists.

The review of the literature[7,8] shows that a typical PPAR agonist consists of an acidic head attached to an aromatic scaffold, a linker, and a hydrophobic tail. In continuation of our studies on indole-based PPAR agonists, the indole was retained as a core skeleton for the acidic head, placing the acetic acid group at the 1-position.[9] The aliphatic linker length was fixed at three carbons on the basis of our previous observations and literature reports.[9−11] A library of compounds was synthesized by selecting various hydrophobic commercially available building blocks. The building blocks **11** and **15** (Figure 2) were short listed after preliminary in vitro screening. Sahoo et al.[10,11] have reported improvement in PPAR$\gamma$ agonist activities upon introduction of a propyl group in the hydrophobic tail. On similar lines the *n*-propyl group was introduced at an ortho position to

* To whom correspondence should be addressed. S.-Y. Wu: phone: 886-37-246-166 ext. 35713; fax: 886-37-586-456; e-mail: suying@nhri.org.tw; H.-P. Hsieh: phone: 886-37-246-166 ext. 35708; fax: 886-37-586-456; e-mail: hphsieh@nhri.org.tw.

[†] National Health Research Institutes.

[‡] Department of Chemistry, National Tsing Hua University.

[§] Graduate Institute of Life Sciences, National Defense Medical Center.

[◇] Department of Life Sciences, National Tsing Hua University.

[#] Department of Chemical Engineering, National Tsing Hua University.

10.1021/jm0510373 CCC: $33.50 
Published on Web 01/14/2006

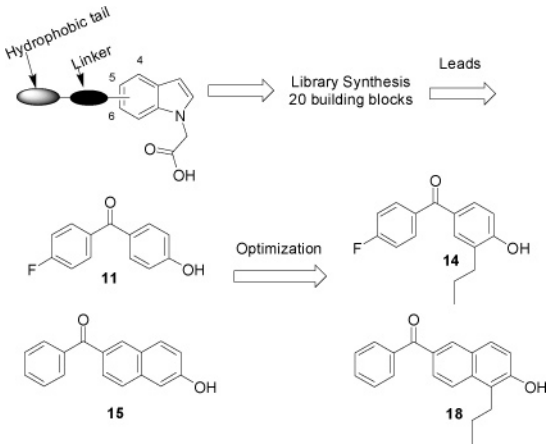


**Figure 2.** Selection and optimization of building blocks for the tail part.

**Scheme 1.** Synthetic Route to **10a**−**l**[a]

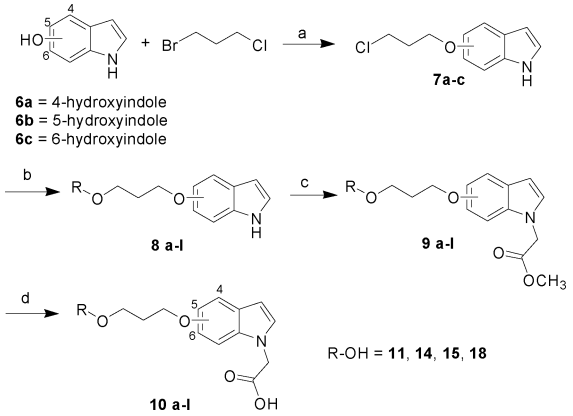


[a] Reagents: (a) KOH, DMSO, rt; (b) R−OH, $K_2CO_3$, KI, DMF, 110 °C; (c) methyl 2-bromoacetate, $K_2CO_3$, KI, ACN; (d) LiOH, MeOH, $H_2O$.

the hydroxyl group in **11** and **15** by Claisen rearrangement to give **14** and **18**, respectively.

**Chemistry.** Compounds **10a**−**l** were synthesized as shown in Scheme 1. The commercially available 4-, 5-, or 6-hydroxy-indoles (**6a**−**c**) were alkylated with 1-bromo-3-chloropropane in the presence of an equimolar amount of potassium hydroxide in DMSO, yielding **7a**−**c**. Compounds **7a**−**c** were coupled with the desired building block **11**, **14**, **15**, or **18** to give **8a**−**l**. The esters **9a**−**l** were obtained by reacting **8a**−**l** with methyl-2-bromoacetate in the presence of potassium carbonate and potassium iodide in acetonitrile. Finally, **9a**−**l** were deprotected with lithium hydroxide in methanol−water mixture to give the desired compounds **10a**−**l**.

## Results and Discussion

The compounds were screened in competitive binding assay[9] and cell-based reporter gene efficacy assay[9] for all three PPAR isoforms, as shown in Table 1. In the benzophenone series, the 5-substituted indole **10b** showed strong binding at PPAR$\gamma$, while its 4- and 6-indole-substituted analogues **10a** and **10c** showed weak binding in the scintillation proximity assay. But **10a**−**c** showed weak or almost no activity in the transactivation assay against all three PPAR subtypes, the only exception being **10c**, which showed sub-micromolar activity as PPAR$\alpha$ agonist. Similarly, the naphthophenone analogue **10h** displayed sub-micromolar affinity in PPAR$\gamma$ and PPAR$\alpha$ binding assays, but its positional analogues **10g** and **10i** showed only weak binding at PPAR$\gamma$. Only 5-substituted indole analogue **10h** showed sub-micromolar activity at PPAR$\alpha$ and micromolar potency of activation at PPAR$\gamma$ in the cell based functional assays.

In an effort to improve the activity, the building blocks **11** and **15** were modified to **14** and **18**, respectively. Compound **10e**, a 5-substituted indole with the *n*-propyl substituted benzophenone tail, displayed sub-micromolar binding as well as functional activity on all three PPAR subtypes. Moving the hydrophobic benzophnone tail to 4-position of indole resulted in a selective PPAR$\alpha$ agonist **10d**. Further, shifting of the linker and hydrophobic benzophenone tail to 6-position of indole **10f** resulted in substantial decrease or loss of activity at all three subtypes. The SARs indicated that 5-substituted indoles might be providing the appropriate distance for the molecule to orient in the binding site to dock the acetic acid group at N1-position of indole in the binding pocket for the acidic head. To confirm

**Table 1.** In Vitro Human PPAR Activities of Indol-1-yl Acetic Acids

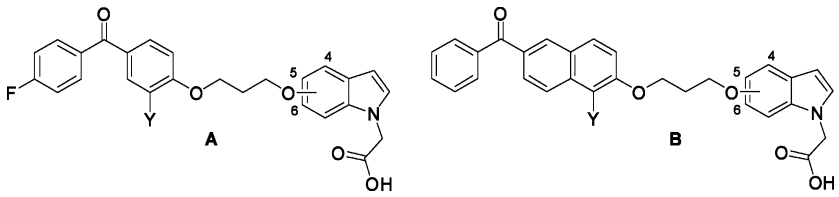


| compd | structure | indole position | Y | SPA $IC_{50}$ ($\mu$M)[a,c] α | SPA $IC_{50}$ ($\mu$M)[a,c] γ | SPA $IC_{50}$ ($\mu$M)[a,c] δ | TA $EC_{50}$ ($\mu$M)[b,c] α | TA $EC_{50}$ ($\mu$M)[b,c] γ | TA $EC_{50}$ ($\mu$M)[b,c] δ |
|---|---|---|---|---|---|---|---|---|---|
| **10a** | A | 4 | H | 1.016 | 2.960 | >10 | >10 | >10 | >10 |
| **10b** | A | 5 | H | >10 | 0.213 | >10 | >10 | 2.160 | >10 |
| **10c** | A | 6 | H | 0.116 | 2.072 | 3.153 | 0.765 | >10 | 4.350 |
| **10d** | A | 4 | *n*-Pr | 0.414 | 2.409 | 3.256 | 0.773 | >10 | 4.000 |
| **10e** | A | 5 | *n*-Pr | 0.470 | 0.129 | 0.649 | 0.050 | 0.160 | 0.610 |
| **10f** | A | 6 | *n*-Pr | 1.047 | 1.287 | 7.616 | >10 | 4.000 | 5.290 |
| **10g** | B | 4 | H | 1.079 | 2.707 | >10 | >10 | >10 | >10 |
| **10h** | B | 5 | H | 0.484 | 0.629 | 4.430 | 0.270 | 1.630 | 5.600 |
| **10i** | B | 6 | H | 4.486 | 1.580 | 2.568 | >10 | >10 | >10 |
| **10j** | B | 4 | *n*-Pr | 0.578 | 0.824 | 5.377 | 0.019 | 2.300 | >10 |
| **10k** | B | 5 | *n*-Pr | 0.113 | 0.050 | 0.223 | 0.008 | 0.070 | 0.500 |
| **10l** | B | 6 | *n*-Pr | 4.486 | 2.024 | 2.398 | 2.475 | 3.870 | 4.900 |
| **1** | | | | >10 | 0.092 | - | - | 0.220 | - |
| **5** | | | | 0.496 | 0.152 | 0.096 | 0.014 | 0.230 | 0.010 |

[a] Concentration of the test compound required to displace 50% of tritiated ligand. [b] Concentration of test compound which produced 50% of the maximal reporter activity. [c] All data within ±15% ($n = 3$).

the role of the indole positions in selectivity, we synthesized the naphthophenone analogues with 4-, 5-, and 6-substituted indoles.

A similar trend was observed in case of naphthophenone analogues. Compound **10k**, with the *n*-propyl-substituted naphthophenone tail attached at the 5-position of indole through a linker, was the most active of all compounds exhibiting potent binding at all three PPAR subtypes and displaying stronger binding and functional activity for PPAR$\gamma$ ($IC_{50}$ = 50 nM, $EC_{50}$ = 70 nM) as compared to rosiglitazone (**1**). It also showed potent PPAR$\alpha$ ($EC_{50}$ = 8 nM) and substantial PPAR$\delta$ ($EC_{50}$ = 500 nM) transactivation potencies. Shifting the naphthophenone hydrophobic tail to the 4-position of indole **10j** gave a PPAR$\alpha$ agonist with 100-fold selectivity over PPAR$\gamma$. Moving the hydrophobic tail to the 6-position of indole **10l** resulted in a substantial decrease in activity at all three subtypes.

The SAR shows that compounds with a hydrophobic tail attached through a linker at the 5-position of the indole exhibited potent activity at all three subtypes. The 4-substitued indoles showed approximately 100-fold selectivity for PPAR$\alpha$ over PPAR$\gamma$, while 6-substituted indoles were inactive or very weak agonists at all three subtypes. The naphthophenone analogue **10k** displayed more potent activity as compared to the benzophenone **10e** as well as benzisoxazole (**5**) analogues, thus indicating that a larger more lipophilic group might be interacting in a better way in the binding pocket for the hydrophobic tail. The addition of the propyl group dramatically enhanced the activity in the functional assay.

A structural biology study was carried out to elucidate the interactions of **10k** with the PPAR$\gamma$ protein. The structure of PPAR$\gamma$ ligand binding domain (LBD) complexed with **10k** was determined to 2.07 Å with the *R* factor of 21.85% and $R_{free}$ of 28.83% (PDB ID 2F4B). PPAR$\gamma$ formed a dimer, and superimposition of one monomer (monomer A) on the other (monomer B) revealed that the difference between the two monomers occurs in the regions of residues 264−273 and residues 468−477. The loop region, residues 264−273, was located at the entrance of the ligand-binding site and was highly flexible in all published structures. The C-terminal region, residues 468−477, was rigid and showed a clear density map in monomer A whereas it was very flexible in monomer B.

Compound **10k** was found bound to monomer A but was absent in monomer B. The stoichiometry of one compound to two monomers was also observed in other published PPAR complex structures.[12,13] The structure of monomer A in complex with **10k** is presented to discuss the interactions between PPAR$\gamma$ and **10k** (Figure 3). The carboxylic acid head of **10k** formed two H-bonds with Tyr473, a residue located in AF-2 helix, and His449. This H-bonding pattern was conserved in most PPAR−agonist complex structures, and in some cases, an additional H-bond was formed with His323 or Ser289.

The indole ring of **10k** formed strong hydrophobic interactions with His449, Cys285, and Phe282. The linker of **10k** was close to the hydrophobic pocket of PPAR consisting of Leu330, Met334, Phe368, Val339, and Met364. Finally, the hydrophobic tail part of **10k** occupied the region near the entrance of the binding pocket and had close contacts with the surrounding residues Met348, Ile341, Leu330, Cys285, Gly284, Glu259, Leu255, and Arg280.

The naphthalene group was sandwiched between Cys285 and Ile341 and made intensive hydrophobic interactions with these two residues, particularly the latter one. The phenyl group in the 6-benzoyl-1-propylnaphthalen-2-yl moiety extended into the hydrophobic site close to the entrance, formed by the Ile249, Val277, Ile341, Leu255, Ile281, and Met348, and made a strong hydrophobic interaction with Leu255. As revealed by the **10k** complex structure, the substitution of a hydrophobic functional group in the phenyl ring is suggested to increase the binding affinity, as it would make additional interactions with Ile249, Ile341, Ile281, or Met348.

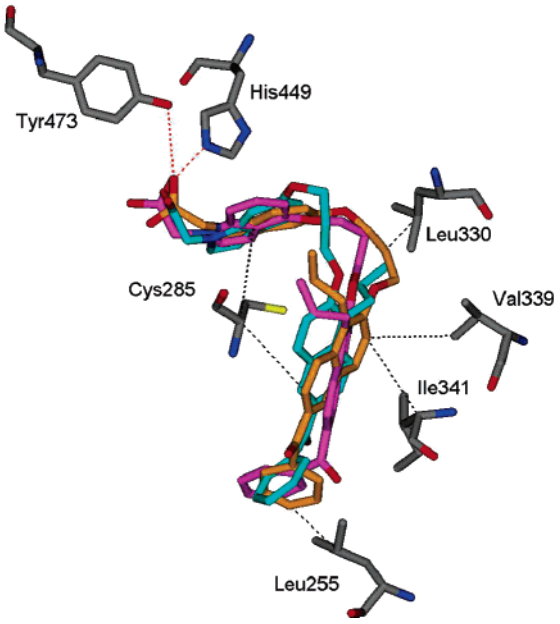


**Figure 3.** Superposition of the crystal structure of **10k** (orange) with docking structures of **10j** (magenta) and **10l** (cyan) in the PPAR$\gamma$ protein. The red and black dotted lines represent hydrogen bond and hydrophobic interactions of **10k** with PPAR$\gamma$ protein, respectively.

**Table 2.** The Distances between the Oxygens in the Acidic Head and Oxygen in the Linker of PPAR Agonists, and Protein−Ligand Intermolecular Energy as Calculated by Insight II

| compd | Ph-O to =O (Å) | Ph-O to OH or NH (Å) | PPAR$\gamma$ $IC_{50}$ ($\mu$M) | PPAR$\gamma$ $EC_{50}$ ($\mu$M) | protein−ligand intermolecular energy (kcal/mol) |
|---|---|---|---|---|---|
| **10j** | 6.4 | 8.0 | 0.824 | 2.300 | −18.5073 |
| **10k** | 7.9 | 8.7 | 0.050 | 0.070 | −57.4929 |
| **10l** | 5.5 | 6.1 | 2.024 | 3.870 | −12.3153 |
| **1** | 8.6 | 9.0 | 0.092 | 0.220 | −56.0647 |
| **3** | 8.6 | 8.8 | 0.001[8] | 0.00028[8] | −59.1996 |

The substantial difference in activities of 5-hydroxy indole analogues as compared to the 4-hydroxy and 6-hydroxy analogues compelled us to study the reasons for it. We decided to study the X-ray cocrystal of **10k** and docking structures for compounds **10j** and **10l**. The molecular docking studies were carried out by docking compounds **10j** and **10l** into the binding pocket of PPAR$\gamma$ using the cocrystal structure of compound **10k** as the template with the program GOLD 2.2.[14] The top pose, ranked by the scoring function, GoldScore, was chosen as the predicted binding mode of compound **10j** and **10l**. The distances between carboxylic acid oxygens and the oxygen on the 4-, 5-, or 6-position of indole in compounds **10j**−**l** were measured to determine whether the positional difference on indole contributed to the difference in activity. These distances were selected because the linker part and the hydrophobic tail were similar for all three molecules and the linker part was quite flexible to maneuver in the binding site; thus, the core skeleton for the acidic head, with different hydroxy indoles, seemed to be the most likely reason for the difference in activity for the three analogues, **10j**−**l**. Table 2 lists the distances between the desired atoms. We also decided to carry out a similar study for X-ray cocrystals of potent PPAR agonists, rosiglitazone (**1**) and

**3** to determine if the distance between acidic group and linker could be criteria for potent PPAR$\gamma$ activity. Compounds **1** and **3** displayed distances between 8 and 9 Å for their acidic part and linker. The X-ray cocrystal of compound **10k**, the most active of all synthesized compounds, with PPAR$\gamma$ also exhibited similar distances between the carboxylic acid oxygens and the oxygen on the 5-position of indole. Shifting the hydrophobic tail to the 4-position (**10j**) decreased the distance between the carboxylic acid and oxygen, correspondingly decreasing the PPAR$\gamma$ agonist activity. Moving the hydrophobic tail to the 6-position in **10l** further decreased the distance and the activity.

Superimposition of docking structures of compound **10j** and **10l** on the crystal structure of **10k** (Figure 3) revealed that the headgroups of these three analogues superimposed well with each other, whereas the linker and the tail parts adopt different conformations. The 5-substituted indole in **10k** allows the best fit to the binding site by providing the optimum distance (8−9 Å) between the carboxylic head and oxygen at the 5-position of indole, thus moving the linker and the hydrophobic tail close to the hydrophobic region of protein consisting of Leu330, Leu333, Val339, Ile341, Met348, and Leu353, resulting in strong hydrophobic interactions with these residues. Decreasing the head−linker distance by shifting the tail to 4-position (**10j**) or 6-position (**10l**) moved the linker and the tail away from this hydrophobic region and consequently weakened the interactions with the protein as revealed by significantly higher protein−ligand intermolecular energy for **10j** and **10l** as compared to **10k** (Table 2). For example, the distances between the tail of **10k** and Val339, Ile341, and Met348 were 3.77, 3.46, and 3.88 Å, respectively, while the tail of **10l** shifted away from Val339, Ile341, and Met348, increasing the distances to 5.29, 4.1, and 4.31 Å, respectively. Thus, the structural biology and the docking studies clearly indicate that distance and placement of the carboxylic group in relation to the oxygen atom on the phenyl ring correlate with the binding affinity of the ligand to the PPAR$\gamma$, and that the 5-substituted indole provides the optimum distance, explaining its better potency as compared to 4- or 6-substituted indoles.

## Conclusion

In conclusion, we have discovered a highly potent PPAR pan-agonist **10k**, with more potent PPAR$\gamma$ agonist activity as compared to rosiglitazone. The structural biology studies reveal strong hydrophobic interactions contributed by the hydrophobic tail 6-benzoyl-1-propylnaphthalen-2-yl, occupying the region near the entrance to the binding pocket. The substitution of a hydrophobic functional group on the phenyl ring of hydrophobic tail may further increase the binding affinity. The molecular docking studies showed that 5-substituted indole provides an appropriate distance to dock the molecule in to the PPAR$\gamma$ binding site to elicit maximum activity. The distances between the acidic group and the linker, when a ligand was complexed with PPAR$\gamma$ protein, were important for the potent activity.

## Experimental Section

**5-(3-Chloropropoxy)-1*H*-indole (7b).** A mixture of 5-hydroxyindole (**6b**) (0.500 g, 3.76 mmol), powdered potassium hydroxide (0.211 g, 3.76 mmol), and DMSO (10 mL) was stirred at room temperature for 10 min, and then 1-bromo-3-chloropropane (0.590 g, 3.76 mmol) was added. The mixture was stirred at room temperature for 0.5 h, and then 15 mL of water was added. The mixture was extracted with ethyl acetate (2 × 30 mL). The combined organic layer was washed with water (6 × 25 mL) followed by brine (2 × 20 mL) and dried over anhydrous $Na_2SO_4$. The solvent was removed in vacuo and the residue flash chromatographed over silica gel eluting with hexane:ethyl acetate (95:5) to give 5-(3-chloropropoxy)-1*H*-indole **7b** (0.631 g, 80%) as a colorless oil. $^1$H NMR (300 MHz, $CDCl_3$) $\delta$ 2.21−2.29 (m, 2H), 3.77 (t, $J$ = 6.3 Hz, 2H), 4.14 (t, $J$ = 6.3 Hz, 2H), 6.46 (m, 1H), 6.84 (dd, $J$ = 2.4, 9.0 Hz, 1H), 7.11 (d, $J$ = 2.1 Hz, 1H), 7.17 (t, $J$ = 2.1 Hz, 1H), 7.26 (d, $J$ = 9.0 Hz, 1H), 8.05 (br, 1H); MS (ESI $m/z$) 210.1 $(M + H)^+$.

Compounds **7a** and **7c** were prepared in similar manner starting from **6a** and **6c**, respectively.

**5-[3-(6-Benzoyl-1-propylnaphthalen-2-yloxy)propoxy]-1*H*-indole (8k).** A mixture of **7b** (0.100 g, 0.48 mmol), **18** (0.139 g, 0.48 mmol), potassium carbonate (0.099 g, 0.72 mmol), and potassium iodide (0.016 g, 0.10 mmol) in 5 mL of DMF was heated at 110 °C for 2 h. The mixture was cooled to room temperature and quenched with water (10 mL). The mixture was extracted with ethyl acetate (2 × 20 mL). The combined organic layer was washed water (6 × 20 mL) followed by brine (2 × 20 mL) and then dried over anhydrous sodium sulfate. The solvent was removed in vacuo to give an oily residue, which was filtered through a short silica column eluting with hexane:dichloromethane (50:50) to give compound **8k** (0.165 g, 75%). $^1$H NMR (300 MHz, $CDCl_3$) $\delta$ 1.01 (t, $J$ = 7.4 Hz, 3H), 1.57−1.70 (m, 2H), 2.29−2.38 (m, 2H), 3.08 (t, $J$ = 7.5 Hz, 2H), 4.27 (t, $J$ = 6.0 Hz, 2H), 4.35 (t, $J$ = 6.0 Hz, 2H), 6.45 (t, $J$ = 2.1 Hz, 1H), 6.86 (dd, $J$ = 2.4, 9.0 Hz, 1H), 7.13 (d, $J$ = 2.1 Hz, 1H), 7.18 (t, $J$ = 2.7 Hz, 1H), 7.27 (d, $J$ = 9.0 Hz, 1H), 7.33 (d, $J$ = 8.7 Hz, 1H), 7.49 (m, 2H), 7.58 (d, $J$ = 7.5 Hz, 1H), 7.76 (d, $J$ = 8.7 Hz, 1H), 7.83 (d, $J$ = 6.6 Hz, 2H), 7.92 (dd, $J$ = 1.8, 9.0 Hz, 1H), 8.01 (d, $J$ = 9.0 Hz, 1H), 8.04 (br, 1H), 8.19 (d, $J$ = 1.8 Hz, 1H). MS (ESI $m/z$) 486.1 $(M + Na)^+$.

Compounds **8a**−**j** and **8l** were synthesized in similar manner starting from appropriate starting materials selected from **7a**−**c**.

**Methyl 2-{5-[3-(6-Benzoyl-1-propylnaphthalen-2-yloxy)propoxy]indol-1-yl}ethanoate (9k).** A mixture of compound **8k** (0.100 g, 0.22 mmol), methyl-2-bromoacetate (0.098 g, 0.65 mmol, 0.06 mL), potassium carbonate (0.045 g, 0.32 mmol), and potassium iodide (0.007 g, 0.04 mmol) in 15 mL of acetonitrile was heated at reflux for 12 h. The mixture was cooled to room temperature and filtered to remove suspended salts. The solvent was removed in vacuo and residue partitioned between dichloromethane and water. The organic layer was washed water (2 × 20 mL) followed by brine (2 × 20 mL) and then dried over anhydrous sodium sulfate. The solvent was removed and the residue chromatographed over silica gel eluting with hexane:ethyl acetate (95:5) to give methyl 2-{5-[3-(6-benzoyl-1-propylnaphthalen-2-yloxy)propoxy]indol-1-yl}ethanoate (**9k**) (0.079 g, 68%). $^1$H NMR (300 MHz, $CDCl_3$) $\delta$ 1.05 (t, $J$ = 7.4 Hz, 3H), 1.58−1.73 (m, 2H), 2.30−2.39 (m, 2H), 3.09 (t, $J$ = 7.5 Hz, 2H), 3.73 (s, 3H), 4.29 (t, $J$ = 6.0 Hz, 2H), 4.36 (t, $J$ = 6.0 Hz, 2H), 4.69 (s, 2H), 6.46 (d, $J$ = 2.7 Hz, 1H), 6.88 (dd, $J$ = 2.4, 9.0 Hz, 1H), 7.14 (d, $J$ = 2.1 Hz, 1H), 7.20 (t, $J$ = 2.7 Hz, 1H), 7.28 (d, $J$ = 9.0 Hz, 1H), 7.33 (d, $J$ = 8.7 Hz, 1H), 7.50 (m, 2H), 7.58 (d, $J$ = 7.5 Hz, 1H), 7.77 (d, $J$ = 8.7 Hz, 1H), 7.83 (d, $J$ = 6.6 Hz, 2H), 7.93 (dd, $J$ = 1.8, 9.0 Hz, 1H), 8.01 (d, $J$ = 9.0 Hz, 1H), 8.20 (d, $J$ = 1.8 Hz, 1H). MS (ESI $m/z$) 536.2 $(M + H)^+$.

Compounds **9a**−**j** and **9l** were synthesized in similar manner starting from **8a**−**j** and **8l**, respectively.

**2-{5-[3-(6-Benzoyl-1-propylnaphthalen-2-yloxy)propoxy]indol-1-yl}ethanoic Acid (10k).** The mixture of compound **9** (0.075 g, 0.140 mmol) and LiOH (0.013 g, 0.561 mmol) in methanol and water mixture (4:1) was refluxed for 2 h. The solvent was removed in vacuo added 0.5 N HCl to residue and extracted with ether (2 × 20 mL). The combined organic layer was washed with water (2 × 20 mL) followed by brine (2 × 10 mL). The solvent was removed in vacuo and the residue chromatographed over a short column of silica gel eluting with dichloromethane:methanol (98:2) to give 2-{5-[3-(6-benzoyl-1-propylnaphthalen-2-yloxy)propoxy]indol-1-yl}ethanoic acid **10l** (0.062 g, 85%). $^1$H NMR (300 MHz, $CDCl_3$) $\delta$ 1.01 (t, $J$ = 7.4 Hz, 3H), 1.61−1.70 (m, 2H), 2.32−2.38 (m, 2H), 3.07 (t, $J$ = 7.8 Hz, 2H), 4.25 (t, $J$ = 6.0 Hz, 2H), 4.33 (t, $J$ = 6.0 Hz, 2H), 4.80 (s, 2H), 6.45 (d, $J$ = 3.0 Hz, 1H), 6.87 (dd, $J$ = 2.1, 9.0 Hz, 1H), 7.01 (d, $J$ = 3.0 Hz, 1H), 7.08−7.12 (m,

2H), 7.31 (d, $J = 9.0$ Hz, 1H), 7.45−7.51 (m, 2H), 7.56−7.61 (m, 1H), 7.74 (d, $J = 9.0$ Hz, 1H), 7.81−7.83 (m, 2H), 7.91 (dd, $J = 1.8$, 9.0 Hz, 1H), 8.01 (d, $J = 9.0$ Hz, 1H), 8.19 (d, $J = 1.5$ Hz, 1H). HRMS ($FAB^+$ *m*/*z*) 521.2208.

Compounds **10a**−**j** and **10l** were synthesized in similar manner as **10k** starting from **9a**−**j** and **9l**, respectively.

**Acknowledgment.** The authors thank Ms. Hsiao-Wen Edith Chu, Ms. Huai-Tzu Chang, and Ms. Pey-Yea Yang for their administrative support, the staff at the beamline SP12B2 for technical assistance, National Health Research Institutes, Taiwan, and National Science Council of the Republic of China (Grant Nos. NSC 92-2323-B-007-001 and NSC 93-2323-B-007-001) for financial support.

**Supporting Information Available:** Synthesis of **14** and **18**, the $^1$H NMR, HRMS, and HPLC purity data for compounds **10a**−**l**, in vitro biological assays and structural biology studies, X-ray data collection and structure refinement for **10k**/PPAR$\gamma$ complex. This material is available free of charge via the Internet at http://pubs.acs.org.

## References

(1) Wolford, J. K.; Vozarova de Courten, B. Genetic Basis of Type 2 Diabetes Mellitus: Implications for Therapy. *Treat. Endocrinol.* **2004**, *3*, 257−267.
(2) Zimmet, P.; Alberti, K. G.; Shaw, J. Global and Societal Implications of the Diabetes Epidemic. *Nature* **2001**, *414*, 782−787.
(3) Eckel, R. H.; Grundy, S. M.; Zimmet, P. Z. The Metabolic Syndrome. *Lancet* **2005**, *365*, 1415−1428.
(4) Luquet, S.; Gaudel, C.; Holst, D.; Lopez-Soriano, J.; Jehl-Pietri, C.; Fredenrich, A.; Grimaldi, P. A. Roles of PPAR delta in Lipid Absorption and Metabolism: A New Target for the Treatment of Type 2 Diabetes. *Biochim. Biophys. Acta* **2005**, *1740*, 313−317.
(5) Berger, J. P.; Akiyama, T. E.; Meinke, P. T. PPARs: Therapeutic Targets for Metabolic Disease. *Trends Pharmacol. Sci.* **2005**, *26*, 244−251.
(6) Moller, D. E. New Drug Targets for Type 2 Diabetes and The Metabolic Syndrome. *Nature* **2001**, *414*, 821−827.
(7) Willson, T. M.; Brown, P. J.; Sternbach, D. D.; Henke, B. R. The PPARs: from Orphan Receptors to Drug Discovery. *J. Med. Chem.* **2000**, *43*, 527−550.
(8) Shearer, B. G.; Hoekstra, W. J. Recent Advances in Peroxisome Proliferator-Activated Receptor Science. *Curr. Med. Chem.* **2003**, *10*, 267−280.
(9) Mahindroo, N.; Huang, C. F.; Peng, Y. H.; Wang, C. C.; Liao, C. C.; Lien, T. W.; Chittimalla, S. K.; Huang, W. J.; Chai, C. H.; Prakash, E.; Chen, C. P.; Hsu, T. A.; Peng, C. H.; Lu, I. L.; Lee, L. H.; Chang, Y. W.; Chen, W. C.; Chou, Y. C.; Chen, C. T.; Goparaju, C. M. V.; Chen, Y. S.; Lan, S. J.; Yu, M. C.; Chen, X.; Chao, Y. S.; Wu, S. Y.; Hsieh, H. P. Novel Indole-Based Peroxisome Proliferator-Activated Receptor Agonists: Design, SAR, Structural Biology, and Biological Activities. *J. Med. Chem.* **2005**, *48*, 8194−8208.
(10) Koyama, H.; Boueres, J. K.; Han, W.; Metzger, E. J.; Bergman, J. P.; Gratale, D. F.; Miller, D. J.; Tolman, R. L.; MacNaul, K. L.; Berger, J. P.; Doebber, T. W.; Leung, K.; Moller, D. E.; Heck, J. V.; Sahoo, S. P. 5-Aryl Thiazolidine-2,4-diones as Selective PPAR$\gamma$ Agonists. *Bioorg. Med. Chem. Lett.* **2003**, *13*, 1801−1804.
(11) Desai, R. C.; Han, W.; Metzger, E. J.; Bergman, J. P.; Gratale, D. F.; MacNaul, K. L.; Berger, J. P.; Doebber, T. W.; Leung, K.; Moller, D. E.; Heck, J. V.; Sahoo, S. P. 5-Aryl Thiazolidine-2,4-diones: Discovery of PPAR Dual $\alpha/\gamma$ Agonists as Antidiabetic Agents. *Bioorg. Med. Chem. Lett.* **2003**, *13*, 2795−2798.
(12) Ebdrup, S.; Pettersson, I.; Rasmussen, H. B.; Deussen, H. J.; Frost Jensen, A.; Mortensen, S. B.; Fleckner, J.; Pridal, L.; Nygaard, L.; Sauerberg, P. Synthesis and Biological and Structural Characterization of the Dual-Acting Peroxisome Proliferator-Activated Receptor $\alpha/\gamma$ Agonist Ragaglitazar. *J. Med. Chem.* **2003**, *46*, 1306−1317.
(13) Sauerberg, P.; Pettersson, I.; Jeppesen, L.; Bury, P. S.; Mogensen, J. P.; Wassermann, K.; Brand, C. L.; Sturis, J.; Woldike, H. F.; Fleckner, J.; Andersen, A. S.; Mortensen, S. B.; Svensson, L. A.; Rasmussen, H. B.; Lehmann, S. V.; Polivka, Z.; Sindelar, K.; Panajotova, V.; Ynddal, L.; Wulff, E. M. Novel Tricyclic-$\alpha$-alkyloxyphenylpropionic Acids: Dual PPAR$\alpha/\gamma$ Agonists with Hypolipidemic and Antidiabetic Activity. *J. Med. Chem.* **2002**, *45*, 789−804.
(14) *GOLD*, 2.2; CCDC Software Limited, Cambridge, UK, 2004.

JM0510373